X-ray dynamical diffraction from single crystals with arbitrary shape and strain field: A universal approach to modeling

Hanfei Yan* and Li Li

National Synchrotron Light Source II, Brookhaven National Laboratory, Upton, New York 11973, USA

(Received 30 July 2013; revised manuscript received 25 November 2013; published 7 January 2014)

The effects of dynamical diffraction in single crystals engender many unique diffraction phenomena that cannot be interpreted by the kinematical-diffraction theory, yet knowledge of them is vital to resolving a vast variety of scientific problems ranging from crystal optics to strain measurements in crystalline specimens. Although the fundamental dynamical-diffraction theory was established decades ago, modeling it remains a challenge in a general case wherein the crystal has complex boundaries and mixed diffraction geometries (Bragg or Laue). Here, we propose a universal approach for modeling x-ray dynamical diffraction from a single crystal with arbitrary shape and strain field that is based on the integral representation of the Takagi-Taupin equations. Using it, we can construct the solution iteratively via a converging series, independent of the diffraction geometry. Moreover, the integral equations offer additional insights into the diffraction physics that are not readily apparent in its differential counterparts. To demonstrate this approach, we studied the dynamical diffraction from a slab of single crystal with both Bragg and Laue diffraction excited on the entrance boundaries, a problem that is difficult to model by other methods. We also explored the mirage effect caused by the presence of a linear strain field and compared it to the Eikonal theory. Lastly, we derived a dynamical-diffraction equation correlating the structural properties of a particle to its far-field Bragg-diffraction pattern, shedding light on how dynamical diffraction affects these kinematical-diffraction-based inverse techniques for reconstructing the shape and the strain field.

DOI: 10.1103/PhysRevB.89.014104 PACS number(s): 41.50.+h, 61.05.cp, 61.72.Dd, 02.30.Rz

I. INTRODUCTION

X-ray diffraction from crystals not only offers a powerful tool for accurately measuring strain but also is an efficient way to manipulate x rays. For weak diffraction from a small crystal or a heavily strained one, the common kinematical-diffraction theory, viz., the Born approximation that is formulated into a Fourier transform of the crystal's electron-density function, will suffice. However, for strong diffraction, the multiple-wave scattering effect is not negligible, so a more rigorous dynamical-diffraction theory must be employed. The effects of dynamical diffraction cause many of the diffraction phenomena in single crystals [1–3], such as the extinction effect, anomalous transmission (the Borrmann effect), double reflection [4], the mirage effect [5,6], and anomalous translation [7]. On the one hand, they complicate our analyses of data for measuring strain [8,9], in particular for techniques built upon the kinematical-diffraction theory [10–12]. On the other hand, they offer opportunities for novel applications of crystal optics [13–15]. In either case, it is critical to use a modeling approach to evaluate the effects of dynamical diffraction.

The classical dynamical-diffraction theory, proposed by Ewald and later reformulated by von Laue, considers a Bloch wave solution to the Maxwell's equations [1–3]. Although this is a powerful approach, giving a clear physical picture, it is limited to perfect single crystals and a plane-wave solution. Later, Kato extended it to a spherical-wave case [16,17]. A more general theory, the Takagi-Taupin equations (TTE) [18,19], was established decades ago to deal with an arbitrary strain field and an illuminating wave front. The TTE has proven extremely powerful in solving dynamical-diffraction problems, but except in a few cases, only numerical solutions are obtained. While many numerical algorithms have been proposed [20–22], all were based on a finite-difference scheme and have two obvious disadvantages: lack of insights and geometric dependence (Bragg or Laue) for numerical implementation. The former prevents us from clarifying the fundamental physics underlying the dynamical-diffraction effects, and the latter limits their applications for crystals with complex shapes and mixed diffraction geometries. Consequently, whether for theoretical studies or practical applications, there is a strong need for a universal modeling approach that can simulate the effects of dynamical diffraction in a general case while still offering sufficient physical clarity. In this paper, we present such an approach based on an iterative solving procedure.

II. MODELING APPROACH

We start by considering TTE with the two-beam approximation. The wave field inside a crystal can be written as the superposition of two waves, $D_0(\mathbf{r})\exp(i\mathbf{k}_0\cdot\mathbf{r})$ and $D_h(\mathbf{r})\exp(i\mathbf{k}_h\cdot\mathbf{r}-i\mathbf{h}\cdot\mathbf{u})$, that are the transmitted and the diffracted waves, respectively, and that satisfy the following coupled partial-differential equations:

$$\begin{aligned}
\frac{\partial}{\partial s_0}D_0 &= i\frac{\pi}{\lambda}(\chi_0 D_0+\chi_{\bar{h}}D_h)\\
\frac{\partial}{\partial s_h}D_h &= i\frac{\pi}{\lambda}[\chi_h D_0+(w_0+\alpha_h)D_h],\\
k &= 2\pi/\lambda,\quad \mathbf{k}_0=k\hat{\mathbf{s}}_0,\quad \mathbf{k}_h=\mathbf{k}_0+\mathbf{h}=k_h\hat{\mathbf{s}}_h,\\
w_0 &= \left(1-k_h^2/k^2\right)+\chi_0\approx 2\eta\sin(2\theta_B)+\chi_0,\\
\alpha_h &= \frac{\lambda}{\pi}\frac{\partial(\mathbf{h}\cdot\mathbf{u})}{\partial s_h}.
\end{aligned}\tag{1}$$

Here, λ is the wavelength of the incident x ray; θ_B is the Bragg angle of the unstrained crystal calculated from Bragg's law; η is

*Corresponding author: hyan@bnl.gov

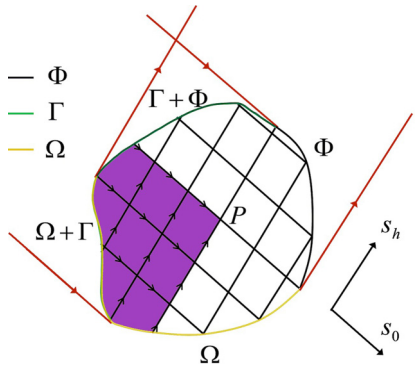

FIG. 1. (Color online) Schematic of x-ray diffraction from a crystal with an arbitrary shape. The oblique coordinates s_0 and s_h represent the incident and diffracted directions, respectively. Boundary conditions need to be satisfied on Γ (green) for the transmitted wave and on Ω (yellow) for the diffracted wave. The diffracted wave exits on Φ (black). The wave field at a point P inside the crystal is only affected by wave fields in the filled region (purple), and the arrows indicate the integration directions in Eq. (3).

the deviation of the incidence angle with respect to the diffracting lattice plane from θ_B; $\mathbf{h}$ is the reciprocal lattice vector of the unstrained crystal; $\mathbf{u}$ is the displacement vector; χ_0, χ_h, and $\chi_{\bar{h}}$ are Fourier coefficients of the susceptibility function of the crystal; and $\hat{\mathbf{s}}_0$ and $\hat{\mathbf{s}}_h$ are the unit vectors along the transmitted and diffracted waves, respectively (Fig. 1). For an incident wave $D_0^{(a)}(\mathbf{r})\exp(i\mathbf{k}_0\cdot\mathbf{r})$, the boundary conditions are

$$D_0(\Gamma) = D_0^{(a)}(\Gamma) \quad \text{and} \quad D_h(\Omega) = 0, \tag{2}$$

where Γ and Ω are the corresponding boundaries for the transmitted and diffracted waves, respectively, composed of the first intersection points of their respective propagation vectors to the crystal's surface (Fig. 1). There is only a unique solution to TTE that fulfills the boundary conditions in Eq. (2). The usual definitions of the Bragg- and Laue-diffraction geometries are distinguished by the boundary conditions. As Fig. 1 shows, if Γ and Ω coincide, it is the Laue geometry; if Γ and Ω do not overlap, it is the Bragg geometry. For situations between, it is a mixed geometry that complicates the calculation.

We first attempt to solve TTE from a purely physical perspective. As stated earlier, the kinematical-diffraction theory neglects the effect of multiple-wave scattering, i.e., the energy interchange between the transmitted and the diffracted waves, and thus is valid only when the diffracted wave is very weak (typically smaller than 0.1, normalized to the incident beam). Consequently, at the kinematical limit, we can set D_h to zero and obtain the analytical expression of the transmitted wave by solving the first equation in Eq. (1). Unsurprisingly, this leads to the well-known exponential transmission function in a medium with the absorption and refraction effects included. Substituting D_0 into the second equation in Eq. (1) yields an analytical expression of D_h that is the kinematical solution of the diffracted wave. The presence of the nonzero D_h accelerates the change of D_0; therefore, we must substitute it back to the first equation to more accurately express the transmitted wave. Accordingly, we also must update the solution to the second equation to reflect the change of the transmitted wave. The iteration continues until a converged solution emerges. At the nth iteration, for a point at $P(s_0,s_h)$, we arrive at

$$\begin{aligned}
D_{0,n}(s_0,s_h) &= D_0^{(a)}\left(s_0^{\Gamma},s_h\right)\exp\left[ic_0\left(s_0-s_0^{\Gamma}\right)\right] \\
&\quad + ic_{\bar{h}}\int_{\Gamma}^{s_0} D_{h,n-1}(s_0',s_h)\exp[ic_0(s_0-s_0')]ds_0', \\
D_{h,n}(s_0,s_h) &= ic_h\int_{\Omega}^{s_h} D_{0,n}(s_0,s_h')\exp\{i\mathbf{h}\cdot[\mathbf{u}(s_0,s_h) \\
&\quad - \mathbf{u}(s_0,s_h')] + ic_w(s_h-s_h')\}ds_h', \\
c_{0,h,\bar{h}} &= k\chi_{0,h,\bar{h}}/2, \quad c_w = kw_0/2, \\
n &= 1,2,3\ldots, D_{h,0}(s_0,s_h) = 0,
\end{aligned} \tag{3}$$

where s_0^{Γ} is the s_0 coordinate of Γ at s_h. This iteration describes and clarifies the interaction between D_0 and D_h. For example, the second integral on the right-hand side of the first equation describes the extinction effect. That is, the transmitted wave attenuates faster than normal absorption because energy is removed from it by the diffracted wave. Due to the uniqueness of the solution, if the iteration converges and the converged solution satisfies the boundary conditions, then it must be the true and only solution to TTE. As is evident from Eq. (3), the integral form of the solution ensures that the boundary conditions are fulfilled automatically, a great advantage compared to approaches based on the finite-difference scheme.

A rigorous proof of convergence can be provided mathematically. Turning the differential equations in Eq. (1) into their integral forms yields

$$\begin{aligned}
D_0(s_0,s_h) &= D_0^{\mathrm{kin}}(s_0,s_h) + \varepsilon\int_{\Omega}^{s_h}\int_{\Gamma}^{s_0} K_0(s_0,s_h;s_0',s_h')D_0(s_0',s_h')ds_0'ds_h' \\
D_h(s_0,s_h) &= D_h^{\mathrm{kin}}(s_0,s_h) + \varepsilon\int_{\Omega}^{s_h}\int_{\Gamma}^{s_0} K_h(s_0,s_h;s_0',s_h')D_h(s_0',s_h')ds_0'ds_h', \\
K_0(s_0,s_h;s_0',s_h') &= \exp\{i\mathbf{h}\cdot[\mathbf{u}(s_0',s_h)-\mathbf{u}(s_0',s_h')] + ic_w(s_h-s_h') + ic_0(s_0-s_0')\}, \\
K_h(s_0,s_h;s_0',s_h') &= \exp\{i\mathbf{h}\cdot[\mathbf{u}(s_0,s_h)-\mathbf{u}(s_0,s_h')] + ic_w(s_h-s_h') + ic_0(s_0-s_0')\}, \quad \varepsilon = -c_hc_{\bar{h}}.
\end{aligned} \tag{4}$$

These are Volterra integral equations of the second kind. Here D_0^{kin} and D_h^{kin} are the kinematical solutions to the transmitted and diffracted waves, respectively, and are the first iterations in Eq. (3). Figure 1 displays the integrated area in purple. Only the wave field inside this region can influence that at P. The iterative solving procedure discussed previously is equivalent

to a Neumann series solution to the Volterra integral equation of the second kind, whose convergence is guaranteed as long as the kernel is square integrable [23].

Because the derivation is similar, here we discuss only the convergence of the iterative solution to the diffracted wave. The Neumann series solution of the diffracted wave can be written as

$$D_{h,M}(s_0,s_h) = \sum_{m=0}^{M} \varepsilon^m \varphi_m(s_0,s_h), \tag{5}$$

where

$$\varphi_m(s_0,s_h) = \int_\Omega^{s_h} \int_\Gamma^{s_0} K_h(s_0,s_h;s_0',s_h')\varphi_{m-1}(s_0',s_h')ds_0'ds_h'.$$

According to Schwartz inequality, we have

$$\begin{aligned}|\varphi_m(s_0,s_h)|^2 &\leqslant \left(\int_\Omega^{s_h}\int_\Gamma^{s_0} |K_h(s_0,s_h;s_0',s_h')|^2 ds_0'ds_h'\right) \\ &\quad\times\left(\int_\Omega^{s_h}\int_\Gamma^{s_0} |\varphi_{m-1}(s_0',s_h')|^2 ds_0'ds_h'\right) \\ &\leqslant S\int_\Omega^{s_h}\int_\Gamma^{s_0} |\varphi_{m-1}(s_0',s_h')|^2 ds_0'ds_h', \\ S &= \int_\Omega^{s_h}\int_\Gamma^{s_0} ds_0'ds_h'. \end{aligned} \tag{6}$$

Integrating Eq. (6) on both sides, we arrive at

$$\begin{aligned}&\int_\Omega^{s_h}\int_\Gamma^{s_0} |\varphi_m(s_0',s_h')|^2 ds_0'ds_h' \\ &\leqslant S\int_\Omega^{s_h}\int_\Gamma^{s_0}\int_\Omega^{s_h'}\int_\Gamma^{s_0'} |\varphi_{m-1}(s_0'',s_h'')|^2 ds_0''ds_h''ds_0'ds_h'. \end{aligned} \tag{7}$$

Integration by parts on the right-hand side of the equation leads to

$$\begin{aligned}&\int_\Omega^{s_h}\int_\Gamma^{s_0} |\varphi_m(s_0',s_h')|^2 ds_0'ds_h' \\ &\leqslant S\int_\Omega^{s_h}\int_\Gamma^{s_0} |\varphi_{m-1}(s_0',s_h')|^2 (s_0-s_0')(s_h-s_h')ds_0'ds_h'. \end{aligned} \tag{8}$$

Combining Eqs. (6) and (8), we can write

$$\begin{aligned}&|\varphi_m(s_0,s_h)|^2 \\ &\leqslant S^2\int_\Omega^{s_h}\int_\Gamma^{s_0} |\varphi_{m-2}(s_0',s_h')|^2 (s_0-s_0')(s_h-s_h')ds_0'ds_h'. \end{aligned} \tag{9}$$

Repeating steps from Eqs. (7) to (9) so that the index in the integral decreases by one every time, we arrive at

$$\begin{aligned}|\varphi_m(s_0,s_h)|^2 &\leqslant \frac{S^m}{[(m-1)!]^2}\int_\Omega^{s_h}\int_\Gamma^{s_0} |\varphi_0(s_0',s_h')|^2 \\ &\quad\times(s_0-s_0')^{m-1}(s_h-s_h')^{m-1}ds_0'ds_h'. \end{aligned}$$

Defining $l_0 = \max(s_0 - s_0')$, $l_h = \max(s_h - s_h')$, and $F^2 = \int_\Omega^{s_h}\int_\Gamma^{s_0} \left|\varphi_0(s_0',s_h')\right|^2 ds_0'ds_h'$, we eventually obtain

$$\left|\varepsilon^m\varphi_m(s_0,s_h)\right| \leqslant \frac{|\varepsilon|^m F}{(m-1)!}\sqrt{l_0^{m-1}l_h^{m-1}S^m}. \tag{10}$$

Because the expression on the right-hand side represents a converging series, the Neumann series solution on the left-hand side also must converge. Earlier, Bremer proposed a similar solving scheme based on the integral equation [Eq. (4)] [24] but did not rigorously discuss the overall convergence of the iterative solution.

III. SIMULATION RESULTS

To demonstrate the capability of our approach, we chose a case wherein an incident plane wave at 12 keV is diffracted from a slab of a perfect Si (004) crystal that is 100 μm thick and 300 μm long. The diffraction geometry differs at different illuminating surfaces [Fig. 2(a)]. There is interest in studying dynamical diffraction in such a case [4,25,26], not only for understanding the fundamental diffraction physics but also for its potential applications in measuring strain with high sensitivity. However, no previous paper has considered the excitation of both the Laue and the Bragg diffractions on the entrance surface due to difficulties in modeling a mixed geometry. With the iterative approach we discuss in this paper, it is straightforward to calculate the diffracted wave, the transmitted wave, and the Poynting vector (energy flow) at different places in the crystal. Figure 2(b)–2(d) show the calculation results at an incident angle of 10 microradians above the Bragg angle. This small amount of deviation accounts for the refraction effect in the Bragg geometry so that the incidence angle is within the total reflection region of the Darwin curve. In the Bragg case, due to the very strong diffraction around the top surface, the energy mostly is

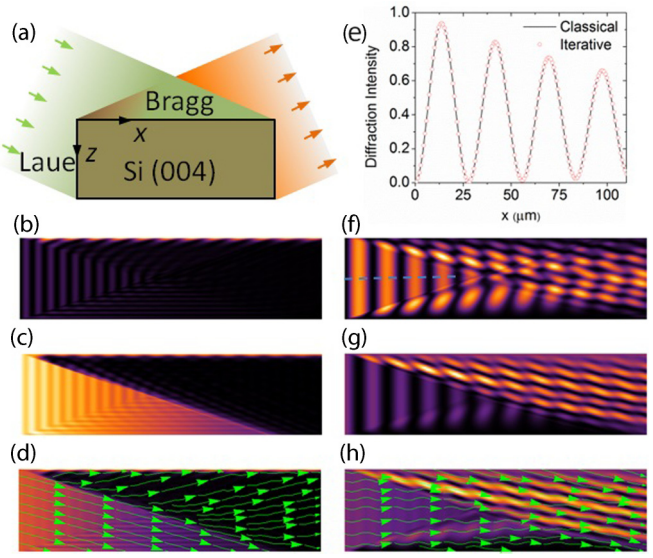

FIG. 2. (Color online) (a) Schematic of a slab of Si (004) crystal illuminated by a plane wave at 12 keV. Dynamical diffraction in Bragg (top incident surface) and Laue (left incident surface) geometries are excited simultaneously. At an incidence angle 10 microradians above the Bragg angle, the simulated results of the (b) diffracted wave, (c) transmitted wave, and (d) Poynting vector (energy flow). The green arrows show the direction of the energy flow. (f)–(h) The same plots when the deviation angle is zero (right at the Bragg angle). (e) The change in diffraction intensity along the dashed line in (f) compared with the classical dynamical-diffraction theory. The oscillation corresponds to the Pendellösung fringes in the Laue case.

confined in a layer not greatly exceeding the extinction depth and can only propagate along the surface [Fig. 2(d)]. Meanwhile, the transmitted wave experiences a strong extinction effect; its intensity quickly decreases to zero at a depth of several microns inside the crystal [Fig. 2(c)]. However, near the left sidewall, the diffraction geometry changes to the Laue case and the phenomenon differs completely. Unlike that in Bragg geometry, the peak of Laue diffraction is centered at the Bragg angle in the symmetric case, not offset by the refraction effect. At this small deviation angle, Laue diffraction is not excited strongly [Fig. 2(b)]. Consequently, energy flows mostly along the incident direction near the left sidewall.

At the exact Bragg angle, in the region of the Laue diffraction, the Pendellösung fringes, viz., the oscillation in diffraction intensity with thickness (here, along the x axis), starts to appear [Fig. 2(f)]. To verify the correctness of the numerical results, we compared the intensity variation along the dashed line in Fig. 2(f) with that calculated from classical dynamical theory [Fig. 2(e)]. They agree perfectly. As we expected, the energy flow in this region is along the diffracting lattice plane. In the Brag-diffraction region, energy no longer propagates along the surface as before but flows along an angle inclined by $\sim 13°$ to the crystal's surface due to the relatively weak diffraction at this incidence angle. As the simulation reveals, a 10-microradian variation in the incidence angle can result in a directional change of more than 10° in energy flow, a phenomenon known as the angular amplification effect in perfect single crystals [1].

Although the individual dynamical-diffraction phenomena discussed herein have been well studied within the framework of the classical dynamical-diffraction theory, the coupling properties of the wave fields generated under two different diffraction geometries remain unresolved. As the simulation demonstrates, the strong interference effect between these two wave fields arises along their geometrical boundaries and then propagates to other regions, engendering profound diffraction-intensity modulations in both the x and the z directions. This fact is of particular importance if the real space variations of the exit diffracted or transmitted wave are of interest.

The crystal we discuss above had no interior strain field. If we were to deform it slightly and introduce a linear strain field, other dynamical-diffraction effects would arise. For weakly deformed crystals, the Eikonal theory that explores the trajectory of the wave field often is employed [27]. Here, we compare the numerical results obtained from the iterative approach with those derived from the Eikonal theory. To better visualize the ray's trajectory, we assumed an incident Gaussian beam with a narrow wave front. The linear strain field has a constant strain gradient of 2.0×10^{-6} μm^{-1}. In Fig. 3(a)–3(c), we plot the variation of the Poynting vector at different incidence angles. The presence of the linear strain field deflects the beam back to the surface, causing a "mirage effect" analogous to that for visible light. However, this phenomenon is associated with the dynamical-diffraction effect, not with refraction. It is the Poynting vector, not the wave vector, that dramatically changes its direction. The energy trajectory follows a hyperbolic curve [28], with the distance separating the two emerging diffraction peaks being determined by the gradient in strain and the incidence angle. We found good agreement between the numerical and the analytical expressions [Fig. 3(d)].

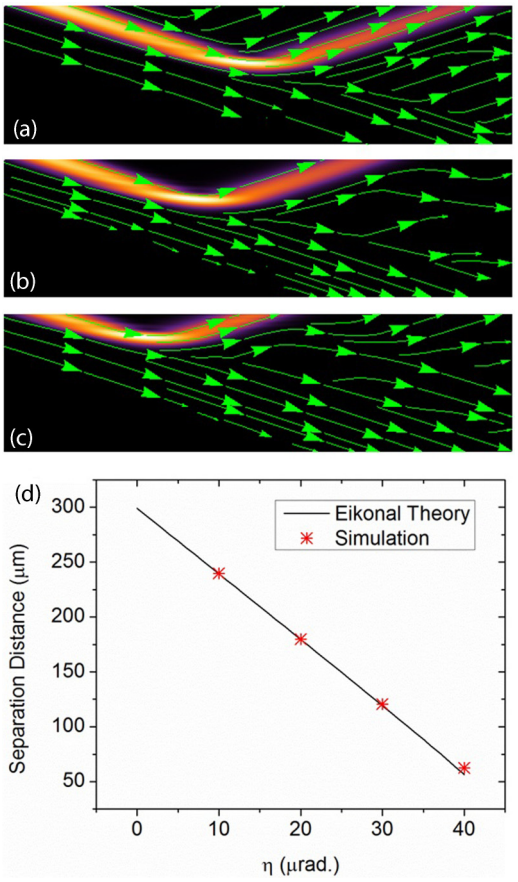

FIG. 3. (Color online) Plots of the Poynting vector (energy flow) when a Gaussian beam is incident on a crystal with a linear strain field along depth z. The green arrows show the direction of the vector. (a)–(c) The deviation angle is 10, 20, and 30 microradians, respectively. The energy flow follows a hyperbolic curve, bending back to the surface due to the presence of the constant strain gradient. The diffracted beam emerges from two locations on the surface separated by a distance dependent upon the deviation angle and the strain gradient. (d) Comparison of the separation distance to the Eikonal theory.

This iterative approach is applicable to any dynamical-diffraction problem where TTE is valid. In particular, for relatively small crystals of less than 10 μm, only a few iterations are needed for convergence of the solution. Therein, not only is the computation faster, but we can derive the approximated analytical expressions.

IV. DYNAMICAL DIFFRACTION IN THE FAR FIELD

In addition its power in terms of numerical calculation, the analytical form of the integral solution in Eq. (3) offers insights into the diffraction physics that are not readily apparent in its differential counterpart. The cases in Figs. 2 and 3 concern the diffraction intensity in real space and on the crystal, but many diffraction problems deal with the pattern of far-field diffraction in reciprocal space. The integral solution allows us to derive the far-field diffraction equation while considering

dynamical diffraction. From the Fresnel-Kirchhoff integral, the expression for the far-field diffracted wave field ϕ_h is derived readily:

$$\phi_h(\Delta\mathbf{q}) \approx A \int\int_{\Phi} \exp(-i\,\Delta\mathbf{q}\cdot\mathbf{r}^{\Phi})(\hat{\mathbf{s}}_h\cdot\mathbf{n})ds \times \int_{\Omega}^{\Phi} D_0 \exp\left[(-i\mathbf{h}\cdot\mathbf{u}) + ic_w\left(s_h^{\Phi} - s_h'\right)\right]ds_h', \quad \Delta\mathbf{q} = \mathbf{k}_d - \mathbf{k}_h. \tag{11}$$

Here, A is a constant of no consequence to this paper, Φ is the emerging surface of the diffracted wave on the crystal, $\mathbf{n}$ is its surface normal, $\mathbf{r}^{\Phi}$ is a position vector on Φ, and $\mathbf{k}_d$ is the receiving wave vector on the detector. We assumed the Fraunhoffer diffraction condition in the derivation. The crystal's volume V is bounded by surfaces Ω and Φ. By noting

$$\int\int_{\Phi}(\hat{\mathbf{s}}_h\cdot\mathbf{n})ds\int_{\Omega}^{\Phi} ds_h' = V$$

and

$$\Delta\mathbf{q}\cdot\hat{\mathbf{s}}_h = \eta k\sin(2\theta_B),$$

we can rewrite Eq. (11) as

$$\phi_h(\Delta\mathbf{q}) = A\int\int\int_V D_0(\mathbf{r})\exp\left\{-i\mathbf{h}\cdot\mathbf{u}(\mathbf{r}) + ik\chi_0\left[s_h^{\Phi}(\mathbf{r}) - s_h'(\mathbf{r})\right]/2\right\}\exp(-i\,\Delta\mathbf{q}\cdot\mathbf{r})d^3r. \tag{12}$$

At first glance, Eq. (12) seemingly is nothing but a Fourier transform. The transformed function includes the phase variation due to the presence of the displacement field, the transmitted wave, and the absorption/refraction correction along the diffracted direction. At the kinematical limit where all effects of absorption, refraction, and multiwave scattering are ignored, it is simplified to the well-known kinematical-diffraction equation

$$\phi_h(\Delta\mathbf{q}) = A\int\int\int_V \exp[-i\mathbf{h}\cdot\mathbf{u}(\mathbf{r})]\exp(-i\,\Delta\mathbf{q}\cdot\mathbf{r})d^3r. \tag{13}$$

Equation (12) illustrates the clear relationship of the far-field diffraction pattern to the crystal's shape, displacement field, and refraction index. It offers an efficient way to evaluate the effects of dynamical diffraction in reciprocal space, as well as clues on how to correct them from the experimental data. One remaining problem in Bragg coherent diffractive imaging (BCDI), which inversely reconstructs the crystal's shape and the strain field by iterative phase-retrieval methods [11,12], is to correct any artifacts from dynamical diffraction, together with those associated with the effects of absorption and refraction. In closely examining Eq. (12), we find that strictly it is not a Fourier transform, since D_0, the transmitted wave, can be a function of $\Delta\mathbf{q}$ when dynamical diffraction is strongly excited. Therefore, the effect of the former on reconstructing the shape and the strain field in BCDI can be profound. Assuming that the transmitted wave only experiences refraction, the usual way of correcting the phase along the incident and diffracted directions [29] readily is deduced as the first-order approximation to Eq. (12). High-order corrections due to the dynamical-diffraction effects are beyond the scope of this paper.

V. SUMMARY

We present a universal approach for modeling x-ray dynamical diffraction from single crystals with arbitrary shape and strain field. We developed it from our observation that we can interpret the interaction between the diffracted and the transmitted waves as an iterative solving process to TTE. We show that this iteration leads to a Neumann series solution to the corresponding integral equation of TTE, and its convergence can be proven rigorously. Compared to other numerical methods based on a finite-difference scheme, this iterative approach yields a solution automatically satisfying boundary conditions, thereby unifying the Bragg- and Laue-diffraction geometries. We verified its correctness in two cases wherein the dynamical phenomena had been studied previously. In addition, the integral solution allows us to derive an analytical expression describing the diffraction intensity in reciprocal space while considering dynamical diffraction. We discussed their effects on Bragg coherent-diffractive imaging. This universal approach will help us to understand many dynamical-diffraction phenomena that remain difficult to model via existing methods and will open opportunities to extend strain-measurement techniques built upon the kinematical-diffraction theory into the dynamical-diffraction regime. In addition, dynamical-diffraction problems for electrons and neutrons can be formulated into a form similar to TTE; therefore, this same methodology likely will be applicable to them.

ACKNOWLEDGMENTS

H.Y. thanks I. K. Robinson for a fruitful discussion on BCDI. This paper was supported by the US Department of Energy, Office of Science, Office of Basic Energy Sciences, under Contract No. DE-AC-02-98CH10886.

[1] A. Authier, *Dynamical Theory of X-Ray Diffraction* (Oxford University Press, Oxford, UK, 2002).
[2] B. W. Batterman and H. Cole, Rev. Mod. Phys. **36**, 681 (1964).
[3] Z. G. Pinsker, *Dynamical Scattering of X-Rays in Crystals* (Springer-Verlag, New York, 1978).
[4] H. F. Yan and I. C. Noyan, J. Appl. Phys. **98**, 073527 (2005).
[5] H. Yan, O. Kalenci, and I. C. Noyan, J. Appl. Crystallogr. **40**, 322 (2007).
[6] H. Yan and I. C. Noyan, J. Appl. Crystallogr. **39**, 320 (2006).
[7] Y. Kohmura, K. Sawada, and T. Ishikawa, Phys. Rev. Lett. **104**, 244801 (2010).
[8] O. Kalenci, C. E. Murray, and I. C. Noyan, J. Appl. Phys. **104**, 063503 (2008).
[9] H. F. Yan, C. E. Murray, and I. C. Noyan, Appl. Phys. Lett. **90**, 091918 (2007).

[10] B. C. Larson, W. Yang, G. E. Ice, J. D. Budai, and J. Z. Tischler, Nature **415**, 887 (2002).
[11] M. A. Pfeifer, G. J. Williams, I. A. Vartanyants, R. Harder, and I. K. Robinson, Nature **442**, 63 (2006).
[12] I. K. Robinson, I. A. Vartanyants, G. J. Williams, M. A. Pfeifer, and J. A. Pitney, Phys. Rev. Lett. **87**, 195505 (2001).
[13] M. F. DeCamp, D. A. Reis, P. H. Bucksbaum, B. Adams, J. M. Caraher, R. Clarke, C. W. S. Conover, E. M. Dufresne, R. Merlin, V. Stoica, and J. M. Wahlstrand, Nature **413**, 825 (2001).
[14] X. R. Huang, D. P. Siddons, A. T. Macrander, R. W. Peng, and X. S. Wu, Phys. Rev. Lett. **108**, 224801 (2012).
[15] Y. Shvyd'ko, S. Stoupin, V. Blank, and S. Terentyev, Nat. Photon. **5**, 539 (2011).
[16] N. Kato, Acta. Cryst. **14**, 627 (1961).
[17] N. Kato, Acta. Cryst. **14**, 526 (1961).
[18] S. Takagi and H. H. Wills, Acta. Cryst. **15**, 1311 (1962).
[19] D. Taupin, Bull. Soc. Fr. Mineral. Crystallogr. **87**, 469 (1964).
[20] Y. Epelboin, Mater. Sci. Eng. **73**, 1 (1985).
[21] J. Gronkowski, Phys. Rep. **206**, 1 (1991).
[22] C. Nourtier and D. Taupin, J. Appl. Crystallogr. **14**, 432 (1981).
[23] G. B. Arfken and H. J. Weber, *Mathematical Methods for Physicists* (Academic Press, San Diego, 1995).
[24] J. Bremer, Acta Crystallogr. A **40**, 283 (1984).
[25] T. Fukamachi, M. Tohyama, K. Hirano, M. Yoshizawa, R. Negishi, D. Ju, K. Hirano, and T. Kawamura, Acta Crystallogr. A **66**, 421 (2010).
[26] S. Jongsukswat, T. Fukamachi, D. Ju, R. Negishi, K. Hirano, and T. Kawamura, J. Appl. Crystallogr. **46**, 1261 (2013).
[27] N. Kato and J. R. Patel, J. Appl. Phys. **44**, 965 (1973).
[28] J. Gronkowski and C. Malgrange, Acta. Cryst. A **40**, 507 (1984).
[29] R. Harder, M. A. Pfeifer, G. J. Williams, I. A. Vartaniants, and I. K. Robinson, Phys. Rev. B **76**, 115425 (2007).